

## **Continuous-Wave and Q-Switched Yb:YSGG Waveguide Laser**

Ma, L.; Tan, Y.; Wang, S.; Akhmadaliev, S.; Zhou, S.; Yu, H.; Zhang, H.; Chen, F.;

Originally published:

December 2016

**Journal of Lightwave Technology 35(2017)13, 2642-2645**

DOI: <https://doi.org/10.1109/JLT.2016.2636221>

Perma-Link to Publication Repository of HZDR:

<https://www.hzdr.de/publications/Publ-25463>

Release of the secondary publication  
on the basis of the German Copyright Law § 38 Section 4.

# Continuous-Wave and Q-Switched YbSGG Waveguide Laser

Linan Ma, Yang Tan, Shuxian Wang, Shavkat Akhmadaliev, Shengqiang Zhou, Haohai Yu, Huaijin Zhang, and Feng Chen, *Senior Member, OSA*

**Abstract**—We report on the continuous-wave and passively Q-switched YbSGG waveguide laser at the wavelength of 1024.8 nm. The ridged waveguide was fabricated on the surface of 100 at. % Yb<sup>3+</sup>-doped YSGG crystal sample (YbSGG) crystal by the swift ion irradiation and the precise diamond blade dicing. Utilizing this waveguide as the gain medium and resonant cavity, the laser emission at 1024 nm was realized. Coating the Tungsten Disulfide onto the waveguide surface as the saturable absorber, the Q-switched laser emission was also obtained with the pulse duration of 125 ns.

**Index Terms**—Rare-earth-doped materials, Waveguides, channeled, Lasers, Q-switched.

## I. INTRODUCTION

WAVEGUIDE laser, as one of basic active devices for the photonic integrated circuits, has a fast development over the past decade [1]-[4]. It is constituted by a waveguide platform in the gain medium. Both the pumping and oscillation laser are confined in the waveguide structure working as the resonant cavity. As the waveguide has a large transverse and longitudinal length ratio, the waveguide laser has a faster thermal dissipation compared with the bulk laser [5]. Meanwhile, the material used for waveguide laser is not limited to the rare earth doped glass and has a broad option. Multiply effective gain materials can be used as the substrate for the waveguide laser, such as the rare earth doped crystal and optical

ceramic [6], [7]. Hence, the waveguide laser has a more compact structure than the fiber laser. Applications and functions of the waveguide laser depend on waveguide fabrication technologies and the selection of the gain medium.

Several technology have been applied for the waveguide fabrication including the proton exchange, ultrafast laser writing, epitaxial growth, ion irradiation and so on. Among them, the ultrafast laser writing [8] and ion irradiation [9] have been proved to be efficient methods to produce the waveguide in multi-materials. Especially for the ion irradiation, until now, kinds of waveguide structures have been fabricated in more than 100 optical materials. Surface waveguides can be easily achieved by the ion irradiation [10], which has an interface with the air. Different from the buried waveguide (inside the optical material), the surface waveguide is more conducive to the heat dissipation and more suitable for the air cooling, indicating a better performance of the waveguide laser.

Rare earth doped garnets, including yttrium aluminum garnet (YAG) [11] and yttrium gallium garnet (YGG) [12], has attracted a continuous attention due to its stable structure, remarkable thermal and optical properties. Recently, a partly disordered crystal of YSGG is developed by randomly substituting scandium for gallium in the octahedral sites of the YGG crystal [13]. Compared to YAG and YGG crystals, YSGG has lower phonon energies. Hence, active ions in YSGG has the reduced multi-phonon decay rates and exhibit a longer fluorescent lifetime of the upper laser level [14]. Besides, the distance between dodecahedral sites can be increased by introducing Sc<sup>3+</sup> ions into YSGG, as radius of Sc is larger than Ga in the octahedral. The increased distance can reduce the relatively strong ion-ion interaction among active ions [15], [16]. Therefore, YSGG allows the high dopant concentration of ytterbium-ions, which is supposed to be more suitable for high-efficiency and Q-switched laser operation.

In the past few years, two-dimensional (2D) material displays outstanding physical and chemical properties [17]-[20]. Recently, Tungsten Disulfide (WS<sub>2</sub>) have joined in the family of the 2D material and attracted intense interests. Similar to MoS<sub>2</sub>, WS<sub>2</sub> is also layered transition metal dichalcogenide. In optics, WS<sub>2</sub> film has the saturable absorption and the broadband nonlinear optics response. It has been utilized as the saturable absorber for Q-switched pulse laser in the fiber and bulk laser system [21], [22].

In this work, the continuous-wave (CW) and Q-switched laser at the wavelength of ~1024 nm were realized in YbSGG

Manuscript received July 9, 2015; revised September 18, 2015, October 30, 2015, and November 16, 2015; accepted November 21, 2015. Date of publication November 23, 2015; date of current version February 10, 2016. This research work is supported by the following funding programs: National Natural Science Foundation of China (Grant No. 11305094 by Y. T.), Young Scholars Program of Shandong University (Grant No. 2015WLJH20 by Y. T.), Fundamental Research Funds for Shandong University (No. 2014JC002), and Helmholtz Association (VH-NG-713 by S. Z.). Ion irradiation was performed at the Ion Beam Center at the Helmholtz-Zentrum Dresden – Rossendorf.

L. Ma, Y. Tan, and F. Chen are with the School of Physics, Shandong University, Jinan 250100, China, and also with the State Key Laboratory of Crystal Materials, Shandong University, Jinan 250100, China (e-mail: malinansdu@163.com; tanyang@sdu.edu.cn; drfchen@sdu.edu.cn).

S. Wang, H. Yu, and H. Zhang are with the State Key Laboratory of Crystal Materials and Institute of Crystal Materials, Shandong University, Jinan 250100, China (e-mail: jrval@usal.es).

S. Akhmadaliev and S. Zhou are with the Helmholtz-Zentrum Dresden-Rossendorf, Institute of Ion Beam and Materials Research, Dresden 01314, Germany (e-mail: author@nrim.go.jp).

Color versions of one or more of the figures in this paper are available online at <http://ieeexplore.ieee.org>.

Digital Object Identifier 10.1109/JLT.2015.2503349

waveguide. The ridged waveguide structure was fabricated on the surface of the YbSGG crystal by the swift carbon ion irradiation and the precise diamond blade dicing. Under the pumping laser at 980 nm, CW laser was observed with maximum output power of 52.3 mW and the slope efficiency of 46%. WS<sub>2</sub> was coated onto the waveguide surface as the saturable absorber. The Q-switched pulse laser was obtained with the minimum pulse duration of 125 ns.

## II. EXPERIMENTS

YbSGG crystal used in this work was grown by the optical floating zone method in a four-ellipsoidal-mirror furnace (FZ-T-12000- X-I-S-SU-Crystal Systems, Inc). The effective segregation coefficient Yb<sup>3+</sup> ions was determined to be 100 at. % measured by x-ray fluorescence (XRF) analysis. The YbSGG crystal was cut into dimensions of 5 × 3 × 3 mm<sup>3</sup> with all facets optically polished. One of the biggest facets was twice irradiated by carbon ion beams. The energy (fluence) of the irradiated carbon beam were 6 MeV (1 × 10<sup>15</sup> ion/cm<sup>2</sup>) and 15 MeV (2 × 10<sup>14</sup> ion/cm<sup>2</sup>), respectively. After irradiation, the planar cladding waveguide was formed near the surface of the irradiated facet.

The planar waveguide was further processed to the ridged waveguide by the precise diamond blade dicing. High-speed spinning (rotate speed 20,000 rpm and the cutting speed 0.1 mm/s) diamond blade cut down the planar waveguide and made grooves onto the surface. Grooves have the width of 20 μm and thickness of 50 μm. Between adjacent grooves, the fragment of the planar waveguide constitute the ridged waveguide. Through controlling the separation distance of grooves, the width of ridged waveguides was adjusted to 40 μm.

Fig. 1 shows the experimental setup for the laser emission in YbSGG waveguide. Two mirrors were adhered onto facets of the YbSGG waveguide as the input (M1) and output (M2) mirrors. The input mirror was coated for high transmission at 940 nm and high reflectance at 1029-1100 nm. While the output mirror has the transmission of 60% at the wavelength of 1029-1100 nm. A diode laser at 940 nm was used as the pump laser. Through a lens (focal distance of 20 mm), the pump laser was coupled into the YbSGG waveguide with the coupling efficiency of 57%. The output laser from the waveguide was collected by a long work microscope objective (MO, N.A.=0.4).

Few-layers WS<sub>2</sub> was transferred into the ethanol and drop-casted onto the surface of the YbSGG waveguide. The drop and drying processes are shown in Fig. 1(b) and (c). Through the interaction with evanescent field of the waveguide mode, the WS<sub>2</sub> film (with the thickness of 30 nm) absorbed the light in the waveguide as the saturable absorber for the Q-switched waveguide laser emission. The Q-switched waveguide laser excitation process is similar to the one shown in Fig. 1(a). The input (output) mirror has high transmission at 940 nm and 99.98% (90%) reflectance at 1029-1100 nm. The pumping laser is coupled into the waveguide through a lens (focal distance of 20 mm) with the coupling efficiency of 57%.

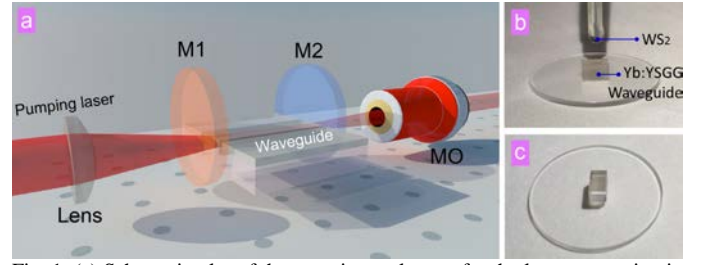


Fig. 1. (a) Schematic plot of the experimental setup for the laser generation in YbSGG waveguide. Inset is the image of the laser oscillation in YbSGG waveguide. Images of the YbSGG waveguide dropped by WS<sub>2</sub> (b) and the dried WS<sub>2</sub> film (c).

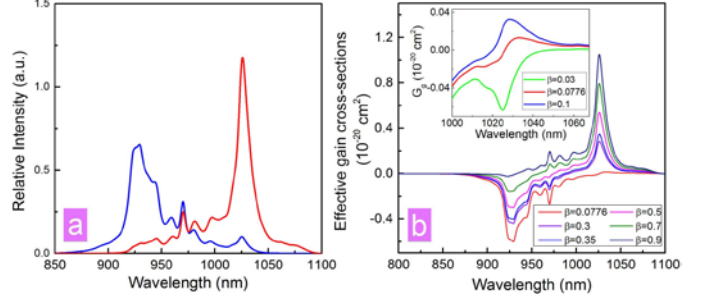


Fig. 2. (a) The absorption and fluorescence (at 300K) spectra of YbSGG versus wavelength. (b)  $\sigma_g$  of YbSGG crystal. The inset is  $\sigma_g$  of YbSGG for  $\beta \leq 0.075$  versus wavelength.

## III. RESULTS AND DISCUSSION

### A. YbSGG crystal characterization:

Fig. 2(a) shows the RT absorption spectra of the YbSGG crystal measured with an excitation laser at the wavelength of 275 nm. As displayed in Fig. 2(a), there is an absorption peak at the wavelength of 929.4 nm with the full-width at half-maximum (FWHM) amounting to 23.2 nm. The broadband absorption demonstrates the advantages of efficient pumping by high-power laser diodes. The RT emission cross-section of the YbSGG crystal is expressed by use of the reciprocity method [24].

$$\sigma_{em}(\lambda) = \sigma_{abs}(\lambda) \frac{Z_l}{Z_u} \exp\left(\left(\frac{h \frac{c}{\lambda_{ZL}} - h \frac{c}{\lambda}}{kT}\right)\right). \quad (1)$$

where  $\sigma_{abs}(\lambda)$  is the absorption cross-section at wavelength  $\lambda$ ,  $Z_l$  and  $Z_u$  are the lower and upper manifold partition functions, respectively.  $h$  is the Planck constant,  $k$  is the Boltzmann constant,  $c$  is the velocity of light, and  $\lambda_{ZL}$  is the wavelength of zero phonon line.  $a = l$  or  $u$ , and  $d_i$  is the degeneracy of the energy level  $E_i$ . According to the Eq. (1), the partition functions  $Z_l$  and  $Z_u$  are calculated to be 1.375 and 1.385, respectively. Peak of the emission spectrum was located at 1026 nm with FWHM of 13 nm corresponding to the transition of  $^2F_{5/2} \rightarrow ^2F_{7/2}$ . Considering about the broadband emission spectrum of YbSGG crystal, YbSGG has the potential to be used as the gain medium for the wavelength tunable laser emission.

The wavelength variation of the oscillated laser can be attributed to the evolution of the effective gain cross-section

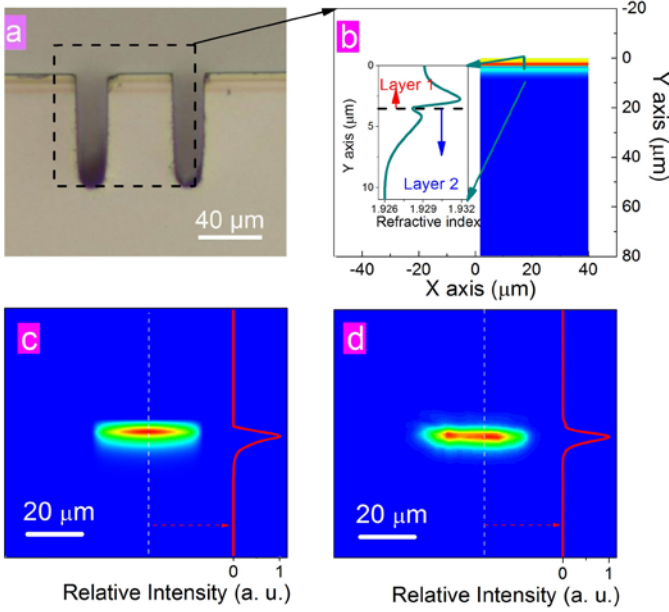


Fig. 3. (a) The image of the YbSGG under pumping. (b) Output power of the waveguide laser as a function of the pumping power. Inset is the spectrum of the output laser.

$(\sigma_g(\lambda))$  of YbSGG crystal, which is expressed as below:

$$\sigma_g(\lambda) = \beta\sigma_{em}(\lambda) - (1 - \beta)\sigma_{abs}(\lambda). \quad (2)$$

$$\beta_{min}(\lambda) = \frac{\sigma_{abs}(\lambda)}{\sigma_{abs}(\lambda) + \sigma_{em}(\lambda)}. \quad (3)$$

Where  $\beta$  is the fraction of  $\text{Yb}^{3+}$  ions excited to the upper manifold;  $\beta_{min}$  is the minimum inversion rate;  $\sigma_{abs}(\lambda)$  is the absorption cross-section and the cavity loss at the wavelength  $\lambda$ ;  $\sigma_{em}(\lambda)$  is the emission cross-section at the wavelength  $\lambda$ .

Fig. 2(b) presents the shift of the peak position of  $\sigma_g(\lambda)$  along with  $\beta_{min}$ . With the increasing of  $\beta_{min}$ , the peak of  $\sigma_g(\lambda)$  has the blue shift. While, with the value of  $\beta_{min}$  above 0.35, the wavelength of the laser is fixed at 1026 nm, which are also observed in Yb:CaGB, Yb:CYB and Yb:YAG crystals [23]. As  $\beta_{min}$  demonstrate the minimum inversion rate of a laser system decided by the balance of  $\sigma_{em}(\lambda)$  and  $\sigma_{abs}(\lambda)$  in Eq. (3). It implies that the laser wavelength can be shifted by changing the cavity loss ( $\sigma_{abs}(\lambda)$ ).

### B. YbSGG waveguide:

Fig. 3(a) shows the microscope image of the YbSGG waveguide cross section. Ridged waveguides have the width of 40  $\mu\text{m}$ . The waveguide has multi-layer due to multiply carbon beam irradiation with different energies. The refractive index profile of the waveguide was displayed in Fig. 3(b) by the intensity profile fitting method (IPFM) [10] at the wavelength of 1024 nm. As one can see, the refractive index distribution has a ladder-like shape which constituted a cladding waveguide structure. Layer 1 with the maximum refractive index worked as the core. Layer 2 and substrate corresponded to the inner and outer cladding. According to the refractive index distribution in Fig. 3(b), the intensity distribution of the propagation mode was

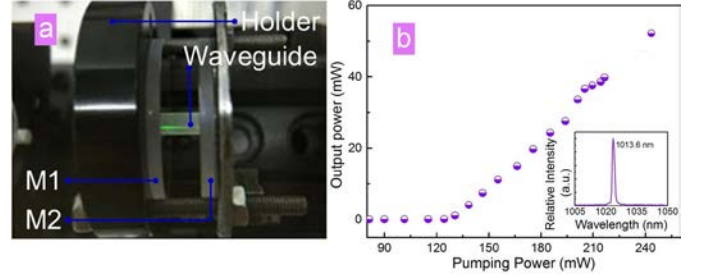


Fig. 4. (a) The image of the YbSGG under pumping. (b) Output power of the waveguide laser as a function of the pumping power. Inset is the spectrum of the output laser.

simulated and shown in Fig. 3(c), which has a good agreement with the measured one in Fig. 3(d).

The cladding waveguide provides several advantages for the laser oscillation. First, as the light was confined in the core with a smaller dimension, the energy density of the propagation mode in the cladding waveguide was higher, which may decrease the laser threshold and increase the slope efficiency of the laser emission. Second, the evanescent field of the propagation mode would be strong, as the position of the peak intensity of the propagation mode is near the surface (Fig. 3(d)). Therefore, the propagation mode will have a better interaction with the coated saturable absorber ( $\text{WS}_2$  film) through the evanescent field [10].of authors which appear at the end of our papers.

### C. CW and Q-switched waveguide laser emission:

Without the  $\text{WS}_2$  film, CW laser emission was observed from the YbSGG waveguide, under the pumping of a 940 nm laser. The image of the YbSGG under pumping is shown in Fig. 4(a). Fig. 4(b) displays the power of the output laser as a function of the pumping power. The maximum output power is 52.3 mW corresponding to the pumping power of 243.4 mW. The slope efficiency and the threshold are 46% and 130.5 mW, respectively. The inset on the right shows the laser emission spectrum of the output laser (solid purple line). The peak position is located at the wavelength of 1023.6 nm.

Adding the  $\text{WS}_2$  onto the surface of YbSGG waveguide, the pulsed laser emission was obtained. The spectrum of the output laser is shown in the inset of Fig. 5(a), demonstrating the laser oscillation at 1024.8 nm. The output power has an exponential variation along with the pump power as displayed in Fig. 5(a) (fitted by the first-order decay exponential function). The laser threshold is 140 mW and the maximum output power 7.8 mW at the highest available incident pump power of 227 mW. The significant decreasing of the output power was induced by the extra-loss from  $\text{WS}_2$  film. Stable pulse laser emission was obtained with the pumping power above 160 mW as shown in Fig. 5(b). Fig. 5(d) displayed variations of the pulse duration and the repetition rate along with the pumping power. The pulse duration was slowly decreased from 175 ns to 125 ns. While, the repetition rate was around 360 kHz ( $\pm 10$  kHz).

Please note, the wavelength of the Q-switched laser (1023.6 nm) has the blue shift compared with the CW laser (1024.8 nm). As the  $\text{WS}_2$  introduced extra-loss into the YbSGG, which decreased the value of  $\beta$ . According to Eq. (2), the peak position of the effective gain cross-section will move to shorter wavelength.



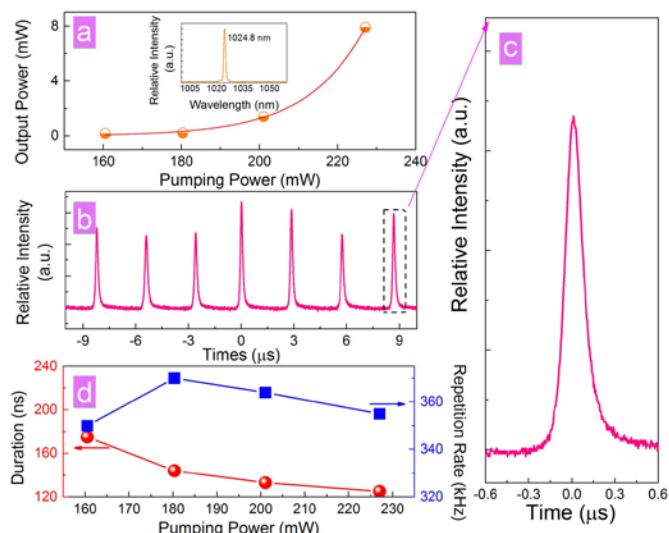


Fig. 5. (a) Output powers of the Q-switched waveguide laser as a function of the absorbed power at 980 nm and the inset illustrates the pulse laser spectrum. The pulse train of pulse laser (b) and an individual laser pulse profile (c) with the pumping power of 227 mW, (d) Variation of the pulse duration and the repetition rate of the Q-switched pulse waveguide laser as a function of the pumping power.

#### IV. -CONCLUSIONS

We report on the continuous-wave and Q-switched laser emission from the YbSGG waveguide. The ridged waveguide was fabricated onto the surface of the YbSGG crystal by the swift ion irradiation. Under the pumping, CW laser emission was obtained with the slope efficiency of 46%. Adding the WS<sub>2</sub> onto the surface of YbSGG waveguide, the pulse laser was also obtained with the pulse duration of 125 ns.

#### REFERENCES

- [1] H. X. Kang, H. Zhang, P. Yan, D. S. Wang, and M. Gong, "An end-pumped Nd:YAG planar waveguide laser with an optical to optical conversion efficiency of 58%," *Laser Phys. Lett.*, vol. 5, no. 12, pp. 879–881, Dec. 2008.
- [2] S. J. Beecher, R. R. Thomson, N. D. Psaila, Z. Sun, T. Hasan, A. G. Rozhin, A. C. Ferrari, and A. K. Kar, "320 fs pulse generation from an ultrafast laser inscribed waveguide laser mode-locked by a nanotube saturable absorber," *Appl. Phys. Lett.*, vol. 97, no. 11, art. no. 111114, Sep. 2010.
- [3] W. Bolanos, F. Starecki, A. Benayad, G. Brasse, V. Menard, J. L. Doualan, A. Braud, R. Moncorge, and P. Camy, "Tm:LiYF<sub>4</sub> planar waveguide laser at 1.9 μm," *Opt. Lett.*, vol. 37, no. 19, pp. 4032–4034, Oct. 2012.
- [4] Y. Tan, C. Cheng, S. Akhmadaliev, S. Q. Zhou, and F. Chen, "Nd:YAG waveguide laser Q-switched by evanescent-field interaction with graphene," *Opt. Exp.*, vol. 22, no. 8, pp. 9101–9106, Apr. 2014.
- [5] F. Chen, "Micro- and submicrometric waveguiding structures in optical crystals produced by ion beams from photonic applications," *Laser Photonics Rev.*, vol. 6, no. 5, pp. 622–640, Sep. 2012.
- [6] Y. Y. Ren, G. Brown, A. Rodenas, S. Beecher, F. Chen, and A. K. Kar, "Mid-infrared waveguide lasers in rare-earth-doped YAG," *Opt. Lett.*, vol. 37, no. 16, pp. 3339–3341, Aug. 2012.
- [7] Y. Tan, H. Zhang, C. J. Zhao, S. Akhmadaliev, S. Q. Zhou, and F. Chen, "Bi<sub>2</sub>Se<sub>3</sub> Q-switched Nd:YAG ceramic waveguide laser," *Opt. Lett.*, vol. 40, no. 4, pp. 637–640, Feb. 2015.
- [8] N. Pavel, G. Salamu, F. Voicu, F. Jipa, M. Zamfirescu, and T. Dascalu, "Efficient laser emission in diode-pumped Nd:YAG buried waveguides realized by direct femtosecond-laser writing," *Laser Phys. Lett.*, vol. 10, no. 9, art. no. 095802, Sep. 2013.

- [9] Y. Tan, S. Akhmadaliev, S. Zhou, S. Sun, and F. Chen, "Guided continuous-wave and graphene-based Q-switched lasers in carbon ion irradiated Nd:YAG ceramic channel waveguide," *Opt. Exp.*, vol. 22, no. 3, pp. 3572–3577, Feb. 2014.
- [10] Z. Shang, Y. Tan, S. Akhmadaliev, S. Q. Zhou, and F. Chen, "Cladding-like waveguide structure in Nd:YAG crystal fabricated by multiple ion irradiation for enhanced waveguide lasing," *Opt. Exp.*, vol. 23, no. 21, pp. 27612–27617, Oct. 2015.
- [11] F. D. Patel, E. C. Honea, J. Speth, S. A. Payne, R. Hutcheson, and R. Equall, "Laser demonstration of Yb<sub>3</sub>Al<sub>5</sub>O<sub>12</sub> (YbAG) and materials properties of highly doped Yb:YAG," *IEEE J. Quantum Electron.*, vol. 37, no. 1, pp. 135–144, Jan. 2001.
- [12] J. H. Zhao, Q. Huang, P. Liu, and X. L. Wang, "An He-implanted optical planar waveguide in an Nd:YGG laser crystal preserving fluorescence properties," *Appl. Surf. Sci.*, vol. 257, no. 16, pp. 7310–7313, Jun. 2011.
- [13] S. X. Wang, K. Wu, Y. C. Wang, H. H. Yu, H. J. Zhang, X. P. Tian, Q. B. Dai, and J. H. Liu, "Spectral and lasing investigations of Yb:YSGG crystal," *Opt. Exp.*, vol. 21, no. 14, pp. 16305–16310, Jul. 2013.
- [14] A. Dening and S. Kück, "Spectroscopy and diode-pumped laser oscillation of Yb<sup>3+</sup>, Ho<sup>3+</sup>-doped yttrium scandium gallium garnet," *J. Appl. Phys.*, vol. 87, no. 9, pp. 4063–4068, May. 2000.
- [15] T. H. Allik, C. A. Morrison, J. B. Gruber, and M. R. Kokta, "Crystallography, spectroscopic analysis, and lasing properties of Nd<sup>3+</sup>:Y<sub>3</sub>Sc<sub>2</sub>Al<sub>3</sub>O<sub>12</sub>," *Phys. Rev. Condens. Matter*, vol. 41, no. 1, pp. B21–B30, Jan. 1990.
- [16] J. Dong, K. Ueda, and A. A. Kaminskii, "Continuous-wave and Q-switched microchip laser performance of Yb:Y<sub>3</sub>Sc<sub>2</sub>Al<sub>3</sub>O<sub>12</sub> crystals," *Opt. Exp.*, vol. 16, no. 8, pp. 5241–5251, Apr. 2008.
- [17] K. F. Mak, C. Lee, J. Hone, J. Shan, and T. F. Heinz, "Atomically thin MoS<sub>2</sub>: a new direct-gap semiconductor," *Phys. Rev. Lett.*, vol. 105, no. 13, art. no. 136805, Sep. 2010.
- [18] Q. H. Wang, K. Kalantar-Zadeh, A. Kis, J. N. Coleman, and M. S. Strano, "Electronics and opto-electronics of two-dimensional transition metal dichalcogenides," *Nature Nanotech.*, vol. 7, pp. 699–712, Nov. 2012.
- [19] M. Chhowalla, H. S. Shin, G. Eda, L. J. Li, K. P. Loh, and H. Zhang, "The chemistry of two-dimensional layered transition metal dichalcogenide nanosheets," *Nat. Chem.*, vol. 5, no. 4, pp. 263–275, Apr. 2013.
- [20] J. A. Miwa, M. Dendzik, S. S. Gronborg, M. Bianchi, J. V. Lauritsen, P. Hofmann, and S. Ulstrup, "Van der Waals epitaxy of two-dimensional MoS<sub>2</sub>-graphene heterostructures in ultrahigh vacuum," *Acs Nano*, vol. 9, no. 6, pp. 6502–6510, Jun. 2015.
- [21] D. Mao, Y. Wang, C. Ma, L. Han, B. Jiang, X. Gan, S. Hua, W. Zhang, T. Mei, and J. Zhao, "WS<sub>2</sub> mode-locked ultrafast fiber laser," *Sci. Rep.*, vol. 5, art. no. 7965, Jan. 2015.
- [22] K. Wu, X. Y. Zhang, J. Wang, X. Li, and J. P. Chen, "WS<sub>2</sub> as a saturable absorber for ultrafast photonic applications of mode-locked and Q-switched lasers," *Opt. Exp.*, vol. 23, no. 9, pp. 11453–11461, May. 2015.
- [23] P. Haumesser, R. Gaumé, B. Viana, and D. Vivien, "Determination of laser parameters of ytterbium-doped oxide crystalline materials," *J. Opt. Soc. Am.*, vol. 19, no. 10, pp. B2365–B2375, Oct. 2002.
- [24] L. D. DeLoach, S. A. Payne, L. L. Chase, L. K. Smith, W. L. Kway, and W. F. Krupke, "Evaluation of absorption and emission properties of Yb<sup>3+</sup>-doped crystals for laser applications," *IEEE J. Quantum Electron.*, vol. 29, no. 4, pp. 1179–1191, Apr. 1993.

**Linan Ma** received the B.S. degree from Taishan University, Taishan, China, in 2015. She is currently working toward the Ph.M. degree at Shandong University, Jinan, China.

Her current research interests include fabrication of optical waveguides in optical crystals by using ion irradiation and optical waveguide amplifier.

**Yang Tan** received the B.S. degree from Shandong Normal University, Jinan, China, in 2013. He is currently working toward the Ph.D. degree at Shandong University, Jinan, China. His current research interests include fabrication of optical waveguides in optical crystals by using femtosecond laser writing.

**Shuxian Wang** be of good quality, professional-looking, and black and white (see above example). Personal hobbies will be deleted from the biography. Following are two examples of an author's biography.

**Shavkat Akhmedaliev** received the B.A. and M.S. degrees from Novosibirsk University in 1994 and 1996 respectively. PhD degree he got from Technical University of Dresden (Germany) in 2004. Since 2004 he is a research scientist at Helmholtz-Center Dresden-Rossendorf. His research activity is concentrated on application of ion beam physics for materials modification and on accelerator mass spectrometry.

**Shengqiang Zhou** received his B.A. and M.S. degrees from Peking Univeristy, Beijing, China, in 1999 and 2002, respectively. He got his Ph.D from Technical University Dresden (Germany) in 2008. Now Dr. Zhou is group leader at Helmholtz-Center Dresden-Rossendorf, Germany. His research focuses on ion beam processed functional materials.

**Haohai Yu**

**Huaijin Zhang**

**Feng Chen** received the B.S. and Ph.D. degrees from Shandong Normal University and Shandong University, Jinan, China, in 1997 and 2002, respectively. In 2002, he was a Lecturer of physics at Shandong University, when he finished his doctoral dissertation on the ion-implanted optical waveguides and their applications in opto-electronics. From 2003 to 2005, he was engaged in research on discrete solitons in nonlinear periodic waveguide arrays or lattices as an Alexander von Humboldt Research Fellow in the Clausthal University of Technology, Germany. In 2004, he became an Associate Professor at Shandong University. In 2006, he became a Professor of physics at Shandong University, where he is currently with the School of Physics and State Key Laboratory of Crystal Materials.

His current research interests include optical waveguides devices produced by energetic ion beam irradiation and ultrafast laser writing, waveguide lasers, and nonlinear optics. Prof. Chen is currently a Senior Member of the Optical Society of America, a Fellow of the Institute of Physics, U.K., and a Director of Chinese Physical Society. He is also an Associate Editor of Optical Engineering and an Editorial Board Member of Scientific Reports.